EXPERIMENTAL IMMUNOLOGY

WILEY [Immunology]

Antigen-specific CD8 T cells in cell cycle circulate in the blood after vaccination

Sonia Simonetti[1,2] | Ambra Natalini[1,2] | Antonella Folgori[3] | Stefania Capone[3] | Alfredo Nicosia[4,5,6] | Angela Santoni[1,2,7] | Francesca Di Rosa[1] (iD)

[1]Institute of Molecular Biology and Pathology, National Research Council (CNR), Rome, Italy

[2]Department of Molecular Medicine, University of Rome "Sapienza", Rome, Italy

[3]Reithera S.r.l., Rome, Italy

[4]Keires AG, Basel, Switzerland

[5]CEINGE - Biotecnologie Avanzate, Naples, Italy

[6]Department of Molecular Medicine and Medical Biotechnology, University of Naples Federico II, Naples, Italy

[7]Istituto Pasteur Italia – Fondazione Cenci Bolognetti, Rome, Italy

Correspondence
Francesca Di Rosa, Institute of Molecular Biology and Pathology, National Research Council (CNR), Rome, Italy.
Email: francesca.dirosa@uniroma1.it; francesca.dirosa@cnr.it

Present address
Sonia Simonetti, Translational Oncology Laboratory, Campus Bio-Medico University, Rome, Italy.

Abstract

Although clonal expansion is a hallmark of adaptive immunity, the location(s) where antigen-responding T cells enter cell cycle and complete it have been poorly explored. This lack of knowledge stems partially from the limited experimental approaches available. By using Ki67 plus DNA staining and a novel strategy for flow cytometry analysis, we distinguished antigen-specific CD8 T cells in G_0, in G_1 and in S-G_2/M phases of cell cycle after intramuscular vaccination of BALB/c mice with antigen-expressing viral vectors. Antigen-specific cells in S-G_2/M were present at early times after vaccination in lymph nodes (LNs), spleen and, surprisingly, also in the blood, which is an unexpected site for cycling of normal non-leukaemic cells. Most proliferating cells had high scatter profile and were undetected by current criteria of analysis, which under-estimated up to 6 times antigen-specific cell frequency in LNs. Our discovery of cycling antigen-specific CD8 T cells in the blood opens promising translational perspectives.

1 | INTRODUCTION

Clonal expansion of T cells during adaptive immune responses is driven by antigen-presenting cells within specialized niches in lymphoid organs, where local chemokines

---

and cytokines guide T cell responses.[1] Although we have learned a great deal about clonally expanding T cells, we still lack essential spatial information, particularly as to the location of T cells during each phase of the cell cycle. This is at least partially due to technical limitations. Classically, flow cytometry data obtained from fresh organ samples containing a heterogeneous mixture of cells have been analysed by in silico gating on antigen-specific CD8 T cells, identified by their ability to bind MHC-antigen multimers. Clonal expansion of antigen-responding CD8 T cells has been assessed by a few methods, including dye-labelling of proliferating cells[2–4] and staining for the intranuclear protein Ki67, after cell fixation and permeabilization.[5–8] To date, available dyes that label cells proliferating over time (eg, CFSE; BrdU) lack the ability to assess whether the labelled cells found in a particular location proliferated locally or rather migrated into that organ after dividing elsewhere. Furthermore, though Ki67 is generally considered to label dividing cells, it actually labels all cells not in G_0. Thus, it does not distinguish actively cycling cells committed to mitosis (those in S-G_2/M) from those in G_1, which may quickly proceed into S, or stay in a prolonged G_1, or even revert to G_0 without dividing.[9]

To study CD8 T cell clonal expansion, we took a slightly different tack: one that is often used by haematologists for cell cycle analysis of bone marrow (BM) haematopoietic stem cells by flow cytometry.[10,11] We used Ki67 plus DNA staining to track rare naïve antigen-specific CD8 T cells responding to vaccination in wild-type mice.[12,13] The naïve CD8 T cells clonally expanded, and we analysed the resulting polyclonal population.

We developed a novel gating strategy to evaluate flow cytometry data that turned out to be a breakthrough in antigen-specific CD8 T cell analysis. We found a significant number of antigen-responding CD8 T cells cycling in lymph nodes (LNs), spleen and —surprisingly—in the blood. Taken together, our results challenge the current flow cytometry guidelines for CD8 T cells at early times of response and open new directions for investigation and intervention in the T cell field.

2 | MATERIAL AND METHODS

2.1 | Adenoviral and MVA vectors

Replication-defective, $\Delta E1$ $\Delta E2$ $\Delta E3$ ChAd3 vector encoding HIV-1 gag protein under HCMV promoter (ChAd3-gag) and Modified Vaccinia Ankara encoding the HIV-1 gag protein under the control of vaccinia p7.5 promoter (MVA-gag) were used in all experiments. ChAd3-gag was generated as described,[14] amplified in human embryonic kidney (HEK) 293 cells, purified by a two-step caesium chloride gradient ultracentrifugation, and titrated by real-time quantitative polymerase chain reaction (PCR). MVA-gag was generated by in vivo recombination in chicken embryo fibroblast (CEF) cells using Red-to-Green gene swapping method and flow cytometry-based cell sorting for isolation of recombinants,[15,16] propagated in CEF cells, purified by centrifugation through sucrose cushion and quantified by plaque assay.

2.2 | Vaccination

Six-week-old female BALB/c mice were purchased from Envigo (S. Pietro al Natisone, Udine, Italy) and housed at Plaisant animal facility (Castel Romano, Rome, Italy). Mice were divided into experimental groups of at least 40 mice each (untreated and vaccinated). All mice of the vaccinated group were primed with ChAd3-gag, and a subset was analysed after priming only. The remaining primed mice were boosted once with MVA-gag, at either day (d) 60 (range 60-67) or d100 (range 95-109) post-prime. Results of d60 and d100 boosts were similar; thus, we combined them. Viral vectors were administered intramuscularly (im) in the quadriceps at a dose of 10^7 viral particles (vp) for ChAd3-gag and 10^6 plaque-forming units (pfu) for MVA-gag, in a volume of 50 μL per side (100 μL total). All experimental procedures were approved by the local animal ethics council and performed in accordance with national and international laws and policies (UE Directive 2010/63/UE; Italian Legislative Decree 26/2014).

2.3 | Organs

Spleen, LNs and blood were obtained at different times after either prime or boost, that is, d7, d10 and d14 post-prime; d3, d7 and d44 post-boost. At each time, the organs were collected from 3 vaccinated and 3 untreated mice, and cells from the 3 mice of each group were pooled. Blood was immediately put into heparin or EDTA blood collection tubes and further processed for analysis. Single-cell suspensions were prepared from spleen and LNs (iliac and inguinal) by mechanical disruption and passage through cell strainers.[17]

2.4 | Membrane staining

Spleen and LN cells were incubated with Fixable Viability Dye conjugated with eFluor780 fluorochrome (Affymetrix, eBioscience, Santa Clara, CA, USA), and background staining was blocked with anti-FcγR mAb (clone 2.4G2). Cells were then incubated for 15 minutes at 4°C with H-2k(d) AMQMLKETI APC-labelled Tetramer (Tetr-gag, NIH Tetramer Core Facility, Atlanta, GA) and PE-labelled Pentamer (Pent-gag, Proimmune, Oxford, UK) to stain for gag$_{197-205}$(gag)-specific CD8 T cells. Cells were incubated for

further 15 minutes at 4°C after addition of the following mAbs: anti-CD3 peridinin chlorophyll protein (PerCP)-Cy5.5 (clone 145-2C11; BD Biosciences, San Jose, CA, USA), anti-CD8α BUV805 (clone 53-6.7, BD Biosciences) and anti-CD62L phycoerythrin (PE)-Cy7 (clone MEL-14, Biolegend, San Diego, CA, USA). Blood samples were incubated for 30 minutes at RT with the above antibodies/reagents that were placed all together. After washing, blood cells were fixed with Cell Fix solution (BD Biosciences). Red cells were lysed with Pharm Lyse solution (BD Biosciences).

2.5 | Intracellular staining

Intracellular staining for Ki67 and DNA was performed as previously described, with some modifications.[10,11] Cells were fixed and permeabilized with Foxp3/Transcription Factor Staining Buffer (Affymetrix, eBioscience). Intracellular staining was performed with anti-Ki67 mAb conjugated with fluorescein isothiocyanate (FITC) or Alexa fluor 700 (clone SolA-15; eBioscience, San Diego, CA, USA). After washing, cells were incubated in PBS with 2 μg/mL Hoechst 33342 (Thermo Fisher Scientific, Waltham, MA, USA) for 15 minutes at RT. After centrifugation at 400 g, cells were resuspended in PBS and analysed by flow cytometry.

2.6 | Flow cytometry analysis

Samples were analysed by LSRFortessa flow cytometer (BD Biosciences) using DIVA software. CD3$^{(-)}$ cells were gated out when acquiring spleen samples. Data were analysed using FlowJo software, v.10 (FlowJo, Ashland, OR, USA).

2.7 | Estimates of gag-specific CD8 T cells in S-G$_2$/M phases of cell cycle

The absolute numbers of gag-specific CD8 T cells in S-G$_2$/M phases of cell cycle in LNs, spleen and blood were estimated based on their percentages determined by flow cytometry and on cell counts. Cells from spleen and LNs were counted by trypan blue exclusion, after lysis of red blood cells. Mouse white blood cell (WBC) counts/μl and total blood volume were previously reported.[18,19]

2.8 | Statistical analysis

The vaccinated group was compared with its corresponding untreated group by performing a two-tailed unpaired Student t test with Welch's correction. A two-tailed paired Student t test was used for comparison of N and R gates. Friedman test with Dunn's multiple comparison was used for comparison of multiple cell subsets within vaccinated

mice samples. Differences were considered significant when *$P \leq 0.05$; **$P \leq 0.01$; ***$P \leq 0.001$. Statistical analysis was performed using Prism v.6.0f, GraphPad Software (La Jolla, CA, USA).

3 | RESULTS

BALB/c mice were vaccinated intramuscularly (im) against the model antigen, HIV-1 gag, using a recombinant chimpanzee-derived adenoviral vector (ChAd3-gag) and a Modified Virus Ankara (MVA-gag) for priming and boosting, respectively. The cell cycle stages of gag-specific CD8 T cells were analysed using Hoechst 33342, a DNA dye and anti-Ki67 mAb.[10,11]

Figure1A-B shows the steps for analysing gag-specific CD8 T cells by flow cytometry, Figure 1B an example of LN cell analysis at day (d) 3 post-boost. Steps 1-2 identify single cells by DNA analysis and live cells by dead cell marker exclusion. Step 3 uses Forward Scatter-A (FSC-A) and Side Scatter-A (SSC-A) profiles to identify certain leucocyte populations. Lymphocytes tend to have low SSC-A and medium-low FSC-A, whereas granulocytes have high SSC-A, and are normally excluded from the canonical "narrow" gate used for lymphocyte studies[20–23] (Figure 1B, Step 3, "narrow"). However, by performing back-gating analysis of gag-specific CD8 T cells from LNs of vaccinated mice, we noticed that the majority of these lymphocytes had high scatter profile and were outside of the "narrow" gate (Figure S1A, top). Furthermore, we noticed an unusual population of cells with high SSC-A that appeared only in spleens of vaccinated mice and contained a significant number of antigen-specific lymphocytes (Figure S1B, black arrow). Thus, we enlarged our FSC-A/SSC-A gate (Figure 1A-B, Step 3 "relaxed"), before gating on CD8 T cells (Step 4) and antigen-specific T cells (Step 5). Back-gating plots and FSC-A/SSC-A profiles of gag-specific CD8 T cells confirmed that the "relaxed" gate was appropriate for our analysis (Figure 1C and Figure S1A, bottom). Remarkably, we found a twofold-sixfold greater proportion of gag-specific CD8 T cells in the "relaxed" gate population than in the "narrow" gate population in both LNs and spleen (Figure 1D-E). Although this gating strategy is novel for standard ex vivo studies of lymphocytes (Figure S2A-B, "narrow" gate at step 3), cells with high FSC-A and high SSC-A are often included when examining in vitro activated T cells.[24] Notably, in current ex vivo studies of lymphocytes, single cells are normally excluded in the FSC-A/FSC-H gate (Figure S2A-B) and less frequently by a two-step gating strategy using FSC-H/FSC-W and SSC-H/SSC-W plots. However, our results show that a high proportion of gag-specific CD8 T cells from LNs of vaccinated mice were outside of these gates (Figure S2C-D).
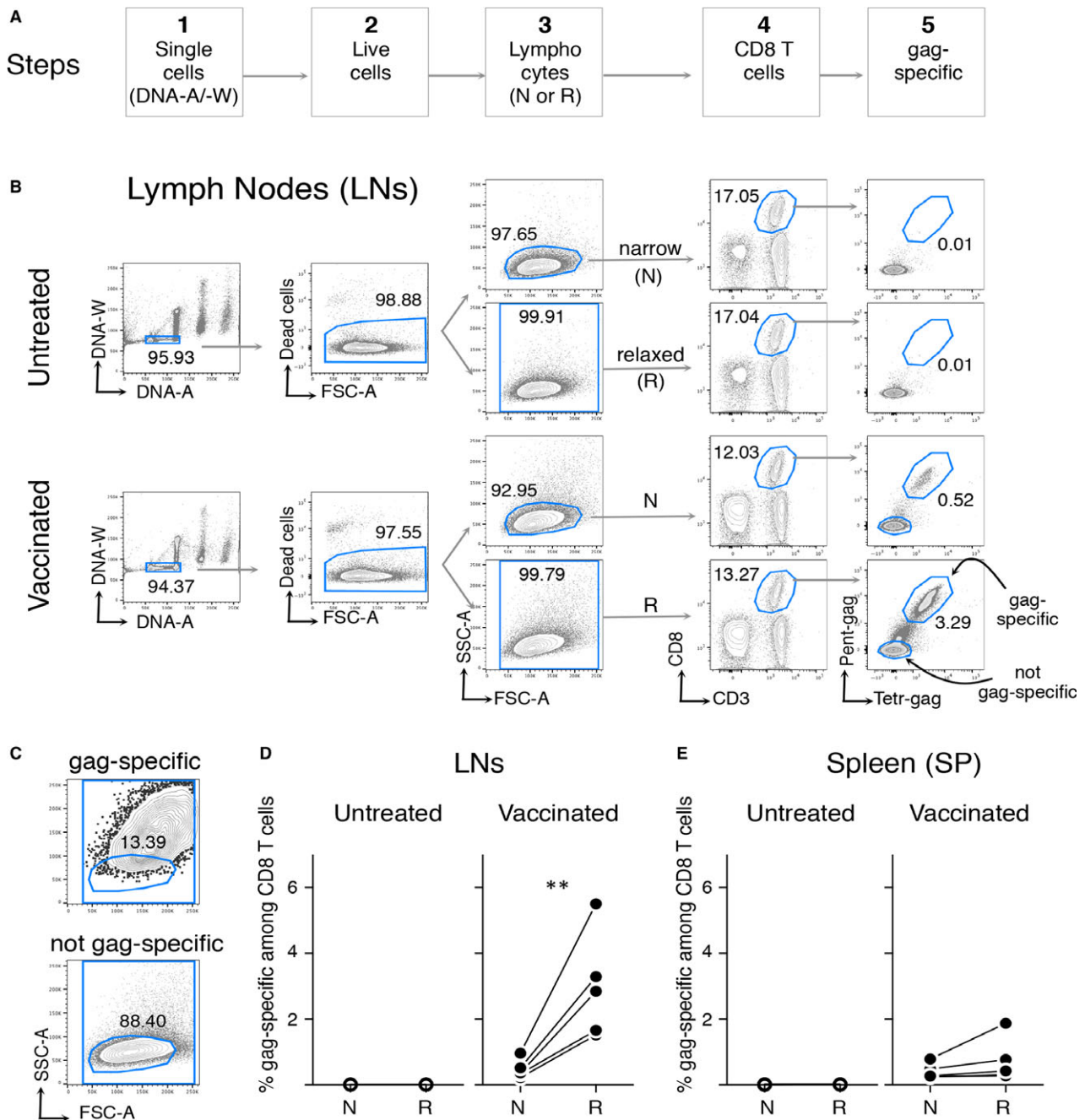
FIGURE 1 Comparison between the narrow (N) and the relaxed (R) gating strategy to evaluate frequency of gag-specific CD8 T cells from lymph nodes (LNs) and spleen (SP) of vaccinated mice at day (d) 3 post-boost. Female BALB/c mice were vaccinated by prime im with ChAd3-gag (10^7 vp) and boost im with MVA-gag (10^6 pfu). Cells from LNs and spleen of vaccinated and untreated mice were analysed by flow cytometry at d3 post-boost. A, Scheme of the gating strategy for analysis of flow cytometry data in 5 steps, to identify the following cells: single cells (Step 1); live cells (Step 2); lymphocytes (Step 3); CD8 T cells (Step 4); and gag-specific cells (Step 5). B, Examples of flow cytometry analysis of cells from LNs of untreated (top) and vaccinated mice (bottom). At step 1, we discriminated single cells from doublets and aggregates by DNA content (DNA-A versus DNA-W). At Step 2, we excluded dead cells by the eFluor780 Fixable Viability Dye. At Step 3, we used either the canonical gate for lymphocyte analysis ("narrow," N) or our proposed gate ("relaxed," R) in the FSC-A/SSC-A plot, as indicated. At Step 4, we gated on $CD3^+$ $CD8^+$ cells, and at Step 5, we evaluated the percentages of gag$_{197-205}$ (gag)-specific cells among them, by combined staining with Pent-gag and Tetr-gag. The numbers represent the percentages of cells in the indicated regions. C, Typical FSC-A/SSC-A plots of gag-specific (top) and not gag-specific (bottom) CD8 T cells from LNs of vaccinated mice at d3 post-boost, analysed using the R gate as in B. D and E, Summary of gag-specific CD8 T cell frequencies in LNs (D) and spleen (E). The Figure summarizes results obtained in 5 prime/boost experiments with a total of 30 mice. Each symbol represents a pool of 3 mice. Statistically significant differences between N and R gates are indicated (**$P \leq 0.01$). Differences in the frequency of gag-specific CD8 T cells between untreated and vaccinated mice were statistically significant both in LNs and spleen, using either R or N gating strategy ($P \leq 0.05$, not shown)

In order to discriminate between gag-specific CD8 T cells in G_0, G_1 and S-G_2/M, we examined Ki67 expression plus DNA content, using either the "narrow" or the "relaxed" gate (Figure 2). We observed a striking difference in the percentages of proliferating cells between the two strategies. The "narrow" gate missed most of the dividing cells in S-G_2/M (<2%), whereas the "relaxed" gate revealed that these cells made up to 42% of the gag-specific cells in LNs and 26% in spleen (Figure 2). Cell cycle entry and progression were accompanied by a graded increase of FSC-A, and more prominently of SSC-A (Figure 2B). In contrast to the gag-specific cells from vaccinated mice, LN and spleen CD8 T cells from untreated mice were almost all in G_0 (average ≥96%). Proliferation was also seen after

a single priming dose, though the kinetics were slower and there were fewer gag-specific cells (Figure S3A-B). The "narrow" gate consistently missed most of the dividing cells and under-estimated antigen-specific CD8 T cell frequency also after priming only (Figure S3C).

In the blood, the "narrow" gate missed up to a third of gag-specific CD8 T cells (Figure S4A), which—with the "relaxed" gate—averaged 2% at d3, 36% at d7% and 13% at d44 post-boost (Figure 3A, C). As expected,[12] gag-specific cells down-modulated CD62L (Figure 3B). A well-defined population of gag-specific CD8 T cells in S-G_2/M was revealed uniquely using the "relaxed" gate (Figure S4B-C). Cells in S-G_2/M were obvious at d3 (up to 13%) and less evident at d7 (0.3%-0.9%) when Ki67^{+}
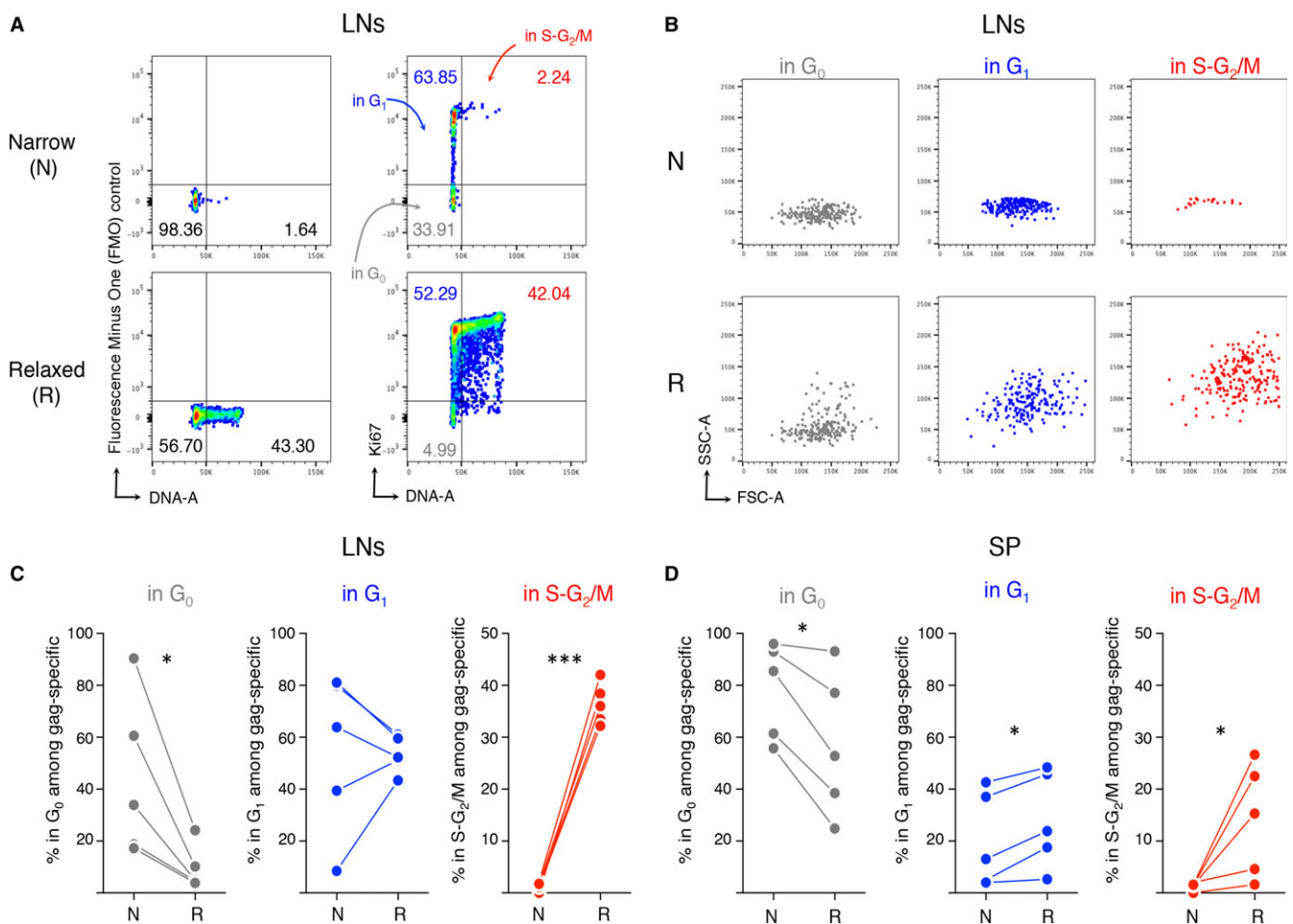

FIGURE 2 Comparison between the narrow (N) and the relaxed (R) gating strategy to evaluate cell cycle of gag-specific CD8 T cells from LNs and spleen of vaccinated mice at d3 post-boost. Female BALB/c mice were vaccinated as in Figure 1. Cell cycle of gag-specific CD8 T cells at d3 post-boost was analysed by Ki67 plus DNA staining, using either the N or the R gate as in Figure 1B. A, Typical DNA/Ki67 staining profiles of LNs, after gating on gag-specific CD8 T cells. Fluorescence Minus One (FMO) controls (left) and Ki67 staining (right) are shown, as indicated. Based on DNA and Ki67 staining, cells in the following phases of cell cycle were identified in the corresponding quadrant: cells in G_0 (Ki67[(−)], 2n DNA), cells in G_1 (Ki67^{+}, 2n DNA) and cells in S-G_2/M (Ki67^{+}, 2n<DNA<4n), as indicated. The numbers represent the percentages of cells in the corresponding quadrant. B, Typical FSC-A/SSC-A plots of LN gag-specific CD8 T cells in G_0, G_1 and S-G_2/M, gated as in A. C and D, Summary of the percentages of gag-specific CD8 T cells in G_0, in G_1 and in S-G_2/M phases in LNs (C) and spleen (D), gated as in A. The Figure summarizes results obtained in 5 boost experiments with a total of 15 vaccinated mice. Each symbol represents a pool of 3 mice. Statistically significant differences are indicated (*$P \leq 0.05$; ***$P \leq 0.001$)
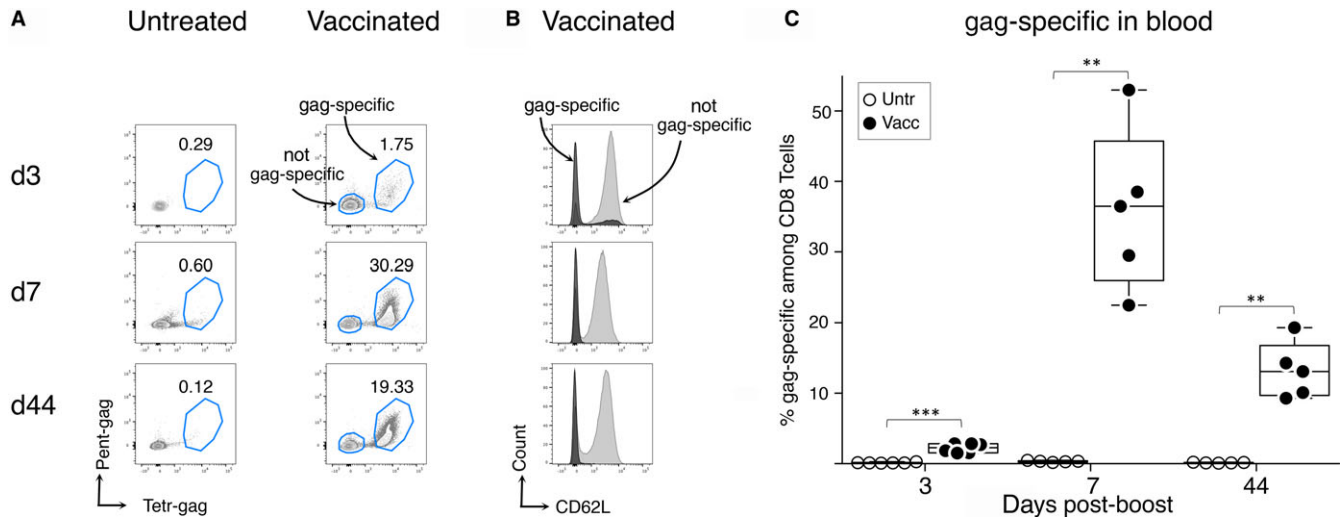
FIGURE 3 Analysis of gag-specific CD8 T cell frequency in the blood of vaccinated mice at d3, d7 and d44 post-boost, using R gate. Female BALB/c mice were vaccinated as in Figure 1. Blood was obtained from untreated and vaccinated mice at d3, d7 and d44 post-boost, and gag-specific CD8 T cells were analysed in 5 steps as in Figure 1A and B, using the R gate at Step 3. A, Typical Pent-gag and Tetr-gag staining profiles of CD8 T cells from untreated (left panels) and vaccinated mice (right panels). The numbers represent the percentages of gag-specific cells in the indicated region, after gating on $CD3^+$ $CD8^+$ cells. B, Example of CD62L membrane expression by gag-specific (black histograms) and not gag-specific (grey histograms) CD8 T cells from vaccinated mice, gated as in A. C, Summary of gag-specific CD8 T cell frequencies in the blood of untreated and vaccinated mice. The Figure summarizes results obtained in 6 prime/boost experiments with a total of 60 mice. Each symbol represents a pool of 3 mice. Statistically significant differences between vaccinated and untreated mice are indicated at each time of analysis (**$P \leq 0.01$; ***$P \leq 0.001$)

peaked ($Ki67^+$ were up to 94%), suggesting that $Ki67^+$ cells (non-G_0) persist in blood after actively proliferating cells disappear (Figure 4). By day 44, almost all gag-specific cells were in G_0 (Figure 4), suggesting that they had mostly switched to a resting memory state. We also saw proliferating antigen-specific CD8 T cells in blood after a single priming shot of vaccine (Figure S5). The proliferating cells in S-G_2/M could be detected only using the "relaxed" gate at both d10 and d14 post-priming (Figure S5).

Taken together, our results show that in blood the average percentages of gag-specific CD8 T cells in S-G_2/M at d3 post-boost and at d10 and d14 after priming were always <5%, about threefold lower and up to 11-fold lower than corresponding percentages in spleen and LNs, respectively (Table 1). We estimated that in the blood the average numbers ±SEM of gag-specific cells in S-G_2/M were 909 ± 418 and 1373 ± 167 at d3 and d7 post-boost, respectively, whereas those in the sum of draining LNs and spleen were $26\,981 \pm 10\,022$ at d3 post-boost (values calculated from data of 5 experiments with a total of 30 vaccinated mice).

Hypothesizing that the increased DNA content of the expanding CD8 T cells could be exploited as a marker to identify proliferating antigen-responding cells in the blood, we focused on $CD62L^{(-)}$ cells, as CD62L is generally down-regulated upon activation (Figure 3B). We evaluated the frequency of gag-specific cells among the following 4 populations of CD8 T cells (Figure 5A): (a) total CD8 T

(including naïve, memory and recently activated cells), (b) $CD62L^{(-)}$ (non-naïve cells), (c) $CD62L^{(-)}$ $Ki67^+$ (non-G_o non-naïve cells) and (d) $CD62L^{(-)}$ in S-G_2/M (dividing non-naïve cells). At d3 post-boost, the average percentage of gag-specific cells among the dividing non-naïve cells was 15-fold higher than among total CD8 T cells (Figure 5C), sometimes up to 70% (Figure 5B), a much higher proportion than observed among the other 3 populations (Figure 5B-C). By d7, the gag-specific cells comprised 40% of the dividing non-naïve and 84% of the non-G_0 non-naïve population. By d44, gag-specific cells were decreased in all the populations, though less evidently in the $CD62L^{(-)}$ population (Figure 5C). At d14 after a single priming dose, gag-specific cells were up to 64% of the dividing non-naïve cells, up to 41% of the non-G_o non-naïve, and <5% in the other 2 populations, suggesting that results after prime were similar to those after boost, though the kinetics slower (Figure S6).

Since CD62L is a cell membrane molecule, and DNA can be visualized using vital dyes, our results suggest that the dividing $CD62L^{(-)}$ CD8 T cells in blood could potentially be a valuable source of live antigen-specific proliferating CD8 T cells at early times of response.

4 | DISCUSSION

Long ago, Sprent & Miller showed that, within days of an immunogenic stimulus, antigen-specific "blast" T cells

FIGURE 4 Cell cycle analysis of gag-specific CD8 T cells in the blood at d3, d7 and d44 post-boost, using R gate. Female BALB/c mice were vaccinated as in Figure 1, and blood samples analysed at d3, d7 and d44 post-boost as in Figure 3A. A, Typical DNA/Ki67 staining profiles of vaccinated mice, after gating on gag-specific CD8 T cells as in Figure 3A. Fluorescence Minus One (FMO) controls (left) and Ki67 staining (right) are shown, as indicated; the numbers represent the percentages of cells in the corresponding quadrant. B, Summary of the percentages of gag-specific CD8 T cells in G_0 (top), in G_1 (middle) and in S-G_2/M (bottom) in the blood of vaccinated mice, compared with corresponding percentages among blood CD8 T cells from untreated controls. The Figure summarizes results obtained in 6 prime/boost experiments with a total of 60 mice. Each symbol represents a pool of 3 mice. Statistically significant differences between vaccinated and untreated mice are indicated at each time of analysis ($*P \leq 0.05$; $***P \leq 0.001$)

circulated in the thoracic duct lymph.[25] There was no way of knowing at that time whether these were actively proliferating cells, or simply activated cells that had left the LNs and were on their way to the blood (the next step in circulation from the thoracic duct). By a novel technical approach, we show here that proliferating antigen-specific T cells circulate in the bloodstream of vaccinated normal mice, challenging the current view that the S-G_2/M phases of clonal expansion occur only in lymphoid organs, or sometimes in BM, or in extra-lymphoid follicles in tissues.[26,27] Thus, proliferation is not always limited to supportive tissues niches, but normal non-leukaemic

lymphocytes that have been stimulated in one organ can expand while circulating to other sites. The contribution of the few cycling cells in the blood to the total pool of proliferating antigen-specific CD8 T cells present in the body is negligible, according to both our calculation and previous estimates.[28,29] Nevertheless, blood might represent an extremely valuable window for analysis of T cell proliferative response, as well as a source of antigen-activated cycling CD8 T cells.

Our findings are in agreement with a previous work performed in a viral infection mouse model, in which proliferation of TCR transgenic anti-viral CD8 T cells was

TABLE 1 Summary of cell cycle analysis of gag-specific CD8 T cells from LNs, spleen and blood at d10 and d14 post-prime, and at d3 post-boost, using R gate

	d10 post-prime		d14 post-prime		d3 post-boost	
	Primed gag-specific	Untreated total CD8	Primed gag-specific	Untreated total CD8	Primed/boosted gag-specific	Untreated total CD8
LNs						
% in G_0	4.69	94.64	4.18	94.44	9.57	96.76
% in G_1	72.44	5.04	79.98	5.12	53.50	2.97
% in $S-G_2/M$	22.88	0.22	15.35	0.28	36.41	0.15
SP						
% in G_0	7.26	93.94	6.67	93.63	57.28	96.03
% in G_1	85.10	5.64	81.33	5.70	28.17	3.41
% in $S-G_2/M$	6.91	0.29	11.87	0.47	14.13	0.32
Blood						
% in G_0	26.75	94.20	25.05	93.80	72.38	95.86
% in G_1	68.75	5.59	69.70	5.84	22.36	3.92
% in $S-G_2/M$	2.05	0.12	4.51	0.15	4.98	0.18

Female BALB/c mice were either vaccinated by prime/boost as in Figure 1, or by prime only as in Figure S3. Cell cycle analysis was performed as in Figure 2, using the R gate. The table shows the average percentages of cells in G_0, in G_1 and in $S-G_2/M$ among gag-specific CD8 T cells from LNs, spleen and blood of vaccinated mice, at the indicated times after prime or boost. The table also shows corresponding percentages among LN, spleen and blood CD8 T cells from untreated controls analysed in parallel. The table summarizes results obtained in 5 prime/boost experiments with a total of 30 mice, and 2 prime experiments with a total of 24 mice.

examined by a 15-minute BrdU pulse plus DNA staining.[4] This study also showed by in vivo microscopy that motile activated/effector CD8 T cells decelerated in virus-infected brain, stopped, and within few minutes divided, documenting a rapid kinetics of cell division and suggesting a link between cell arrest and mitosis/cytokinesis.[4] Although the proposed concept that cytoskeleton dynamics and cell cycle are intertwined is in agreement with other studies,[30,31] one caveat is that high numbers of TCR transgenic cells were adoptively transferred into wild-type mice, thus failing to closely mimic the normal T cell kinetics of response, proliferative expansion and phenotype.[32] Furthermore, S phase was measured by a 15-minute BrdU pulse, leaving open the possibility that the labelled cells found in a particular location had duplicated their DNA elsewhere.

In our study, proliferating gag-specific CD8 T cells in $S-G_2/M$ were found in the blood of normal mice also after a single dose of ChAd3-gag, although they were fewer than after a boost with MVA-gag, as a result of a lower number of total gag-specific cells. Furthermore, slower kinetics of the primary response and/or differences in spatial distribution of antigen-responding CD8 T cells inside the LNs between prime and boost[33] were possibly reflected in the blood. Further studies will be necessary to elucidate whether naïve and memory cells behave differently upon stimulation in vivo, whether vaccination route matters, and whether the cycling CD8 T cell clones in the blood comprise a special highly dividing subset and/or express high-affinity TCRs.

The majority of dividing CD8 T cells in blood, spleen and LNs showed increased FSC-A and unusually high SSC-A, likely due to changes in mitochondria, chromatin condensation, etc.[34,35] Cells with these characteristics are usually excluded from the analysis of normal lymphocytes ex vivo, for example, human blood lymphocytes in conditions apart from cancer. Considering that nearly all immunological studies in humans use blood samples, important information are likely to be missed, perhaps leading to incorrect conclusions. For example, it was found that up to 70% of virus-specific CD8 T cells were Ki67$^+$ in the blood of patients at early phases of primary infections,[6,7] whereas memory-phenotype CD8 T cells from the blood of donors with no apparent infections comprised about 2%-10% of Ki67$^+$ cells .[36] Furthermore, an early increase of Ki67$^+$ PD-1$^+$ CD8 T cells was observed in the blood of a subset of lung cancer patients treated with checkpoint inhibitors, and it was proposed that this could be relevant for antitumor effects.[37] In all these studies, it was suggested that the Ki67$^+$ cells were proliferating in response to a recent immunogenic stimulus;[6,7,36,37] however, cells with high side scatter were discarded,[7,37] and DNA content was not evaluated;[6,7,36,37] thus, it cannot be distinguished whether the Ki67$^+$ were actively cycling, or rather they were non-proliferating cells in G_1, possibly on their way back to G_0. Furthermore, the proliferation—when present—was likely greatly under-estimated. A single study in humans did use DNA staining and found that an average of <0.1% of memory-phenotype CD8 T cells were in $S-G_2/$
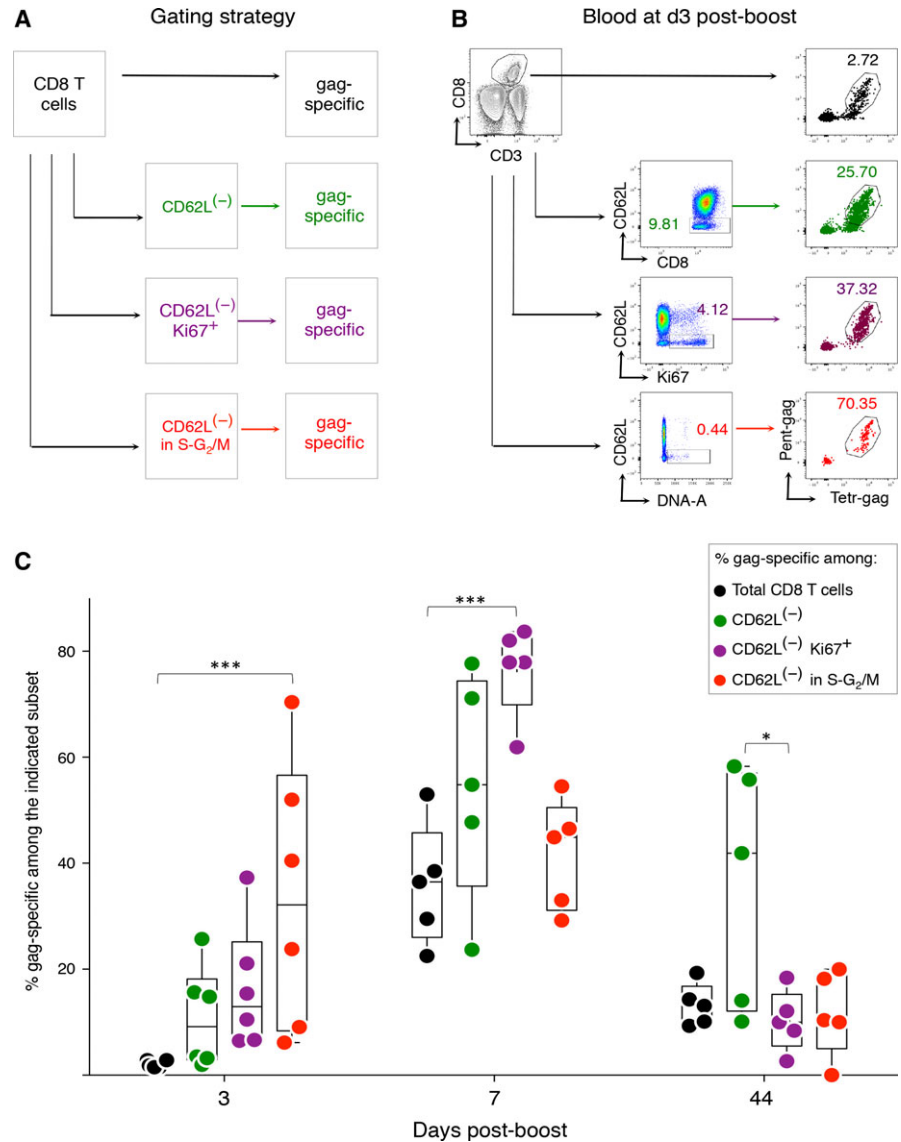
FIGURE 5 Specific enrichment of gag-specific CD8 T cells within a population of CD62L$^{(-)}$ CD8 T cells in S-G$_2$/M in the blood of vaccinated mice at d3 post-boost. Female BALB/c mice were vaccinated as in Figure 1, and blood samples analysed at d3, d7 and d44 post-boost as in Figures 3 and 4, using the R gate. The frequency of gag-specific CD8 T cells among the following cell populations was determined: total CD8 T cells; CD62L$^{(-)}$ CD8 T cells; Ki67$^+$ CD62L$^{(-)}$ CD8 T cells and CD62L$^{(-)}$ CD8 T cells in S-G$_2$/M. A, Gating strategy. B, Example of flow cytometry profiles at d3 post-boost. Numbers represent the percentages of cells in the indicated regions. C, Summary of the results. Statistically significant differences are indicated at each time of analysis (*$P \leq 0.05$; ***$P \leq 0.001$). The Figure summarizes results obtained in 6 prime/boost experiments with a total of 30 vaccinated mice. Each symbol represents a pool of 3 mice

M in the blood of donors with no systemic diseases.[36] The interpretation at that time was that blood-derived memory CD8 T cells are resting.[36,38,39] Our interpretation is instead that the cells in S-G$_2$/M could have been newly activated cells responding to an environmental antigen. We suggest that the widespread use of our technical approach might prevent incomplete data analysis and/or biased interpretations.

Our results have several potential translational uses. For example, human blood might be the source of enriched populations of recently activated CD8 T cells, proliferating in response to vaccines, infections, transplantation and cancers, that could be studied, cloned and used therapeutically, even without knowing the antigen to which they are responding, or as a way of searching for that antigen. And, in cases where a patient presents with symptoms of immune activation, but no obvious infection, an analysis of the CD8 T cells in S-G$_2$/M in the blood could reveal clues as to the cause of the symptoms and/or the target of the response.

CONFLICT OF INTEREST

AF and SC are employees of Reithera Srl. A Nicosia is member of the Board of Directos of Keires AG. A Nicosia is named inventor on patent application WO 2005071093

(A3) "Chimpanzee adenovirus vaccine carriers." Authors do not disclose any other conflict of interest.

AUTHOR CONTRIBUTIONS

ORCID

Francesca Di Rosa 🄳 https://orcid.org/0000-0003-0252-9138

REFERENCES

1. Castellino F, Huang AY, Altan-Bonnet G, Stoll S, Scheinecker C, Germain RN. Chemokines enhance immunity by guiding naive CD8+ T cells to sites of CD4+ T cell-dendritic cell interaction. *Nature*. 2006;440:890-895.
2. Murali-Krishna K, Altman JD, Suresh M, et al. Counting antigen-specific CD8 T cells: a reevaluation of bystander activation during viral infection. *Immunity*. 1998;8:177-187.
3. van Stipdonk MJ, Lemmens EE, Schoenberger SP. Naive CTLs require a single brief period of antigenic stimulation for clonal expansion and differentiation. *Nat Immunol*. 2001;2:423-429.
4. Kang SS, Herz J, Kim JV, et al. Migration of cytotoxic lymphocytes in cell cycle permits local MHC I-dependent control of division at sites of viral infection. *J Exp Med*. 2011;208:747-759.
5. Pandrea I, Gaufin T, Gautam R, et al. Functional Cure of SIVagm Infection in Rhesus Macaques Results in Complete Recovery of CD4+ T Cells and Is Reverted by CD8+ Cell Depletion. *PLoS Pathog*. 2011;7:e1002170.
6. Zaunders JJ. Early proliferation of CCR6+ CD38+++ antigen-specific CD4+ Th1 effector cells during primary HIV-1 infection. *Blood*. 2005;106:1660-1667.
7. van Aalderen MC, Remmerswaal EB, Verstegen NJ, et al. Infection history determines the differentiation state of human CD8+ T cells. *J Virol*. 2015;89:5110-5123.
8. Bolinger B, Sims S, Swadling L, et al. Adenoviral vector vaccination induces a conserved program of CD8(+) T cell memory differentiation in mouse and man. *Cell Rep*. 2015;13:1578-1588.
9. Di Rosa F. Two niches in the bone marrow: a hypothesis on lifelong T cell memory. *Trends Immunol*. 2016;37:503-512.
10. Wilson A, Murphy MJ, Oskarsson T, et al. c-Myc controls the balance between hematopoietic stem cell self-renewal and differentiation. *Genes Dev*. 2004;18:2747-2763.
11. Hirche C, Frenz T, Haas SF, et al. Systemic virus infections differentially modulate cell cycle state and functionality of long-term hematopoietic stem cells in vivo. *Cell Rep*. 2017;19:2345-2356.
12. Quinn KM, Da Costa A, Yamamoto A, et al. Comparative analysis of the magnitude, quality, phenotype, and protective capacity of simian immunodeficiency virus gag-specific CD8+ T cells

following human-, simian-, and chimpanzee-derived recombinant adenoviral vector immunization. *J Immunol*. 2013;190:2720-2735.
13. Stanley DA, Honko AN, Asiedu C, et al. Chimpanzee adenovirus vaccine generates acute and durable protective immunity against ebolavirus challenge. *Nat Med*. 2014;20:1126-1129.
14. Colloca S, Barnes E, Folgori A, et al. Vaccine vectors derived from a large collection of simian adenoviruses induce potent cellular immunity across multiple species. *Sci Transl Med*. 2012;4:115ra2.
15. Di Lullo G, Soprana E, Panigada M, et al. Marker gene swapping facilitates recombinant Modified Vaccinia Virus Ankara production by host-range selection. *J Virol Methods*. 2009;156:37-43.
16. Di Lullo G, Soprana E, Panigada M, et al. The combination of marker gene swapping and fluorescence-activated cell sorting improves the efficiency of recombinant modified vaccinia virus Ankara vaccine production for human use. *J Virol Methods*. 2010;163:195-204.
17. Quinci AC, Vitale S, Parretta E, et al. IL-15 inhibits IL-7Ralpha expression by memory-phenotype CD8(+) T cells in the bone marrow. *Eur J Immunol*. 2012;42:1129-1139.
18. Nemzek JA, Bolgos GL, Williams BA, Remick DG. Differences in normal values for murine white blood cell counts and other hematological parameters based on sampling site. *Inflamm Res*. 2001;50:523-527.
19. Riches AC, Sharp JG, Thomas DB, Smith SV. Blood volume determination in the mouse. *J Physiol*. 1973;228:279-284.
20. Cossarizza A, Chang HD, Radbruch A, et al. Guidelines for the use of flow cytometry and cell sorting in immunological studies. *Eur J Immunol*. 2017;47:1584-1797.
21. Ahmed R, Roger L, Costa Del Amo P, et al. Human stem cell-like memory T cells are maintained in a state of dynamic flux. *Cell Rep*. 2016;17:2811-2818.
22. Yu W, Jiang N, Ebert PJ, et al. Clonal Deletion Prunes but Does Not Eliminate Self-Specific αβ CD8(+) T Lymphocytes. *Immunity*. 2015;42:929-941.
23. Gordon CL, Miron M, Thome JJ, et al. Tissue reservoirs of antiviral T cell immunity in persistent human CMV infection. *J Exp Med*. 2017;214:651-667.
24. Aslan N, Watkin LB, Gil A, et al. Severity of acute infectious mononucleosis correlates with cross-reactive influenza CD8 T-cell receptor repertoires. *MBio*. 2017;8:e01841-17.
25. Sprent J, Miller JF. Interaction of thymus lymphocytes with histoincompatible cells. II. Recirculating lymphocytes derived from antigen-activated thymus cells. *Cell Immunol*. 1972;3:385-404.
26. Siracusa F, McGrath MA, Maschmeyer P, et al. Nonfollicular reactivation of bone marrow resident memory CD4 T cells in immune clusters of the bone marrow. *Proc Natl Acad Sci U S A*. 2018;115:1334-1339.
27. Jones GW, Jones SA. Ectopic lymphoid follicles: inducible centres for generating antigen-specific immune responses within tissues. *Immunology*. 2016;147:141-51.
28. Westermann J, Pabst R. Lymphocyte subsets in the blood: a diagnostic window on the lymphoid system? *Immunol Today*. 1990;11:406-410.
29. Di Rosa F, Pabst R. The bone marrow: a nest for migratory memory T cells. *Trends Immunol*. 2005;26:360-366.
30. Chen W, Zhu C. Mechanical regulation of T-cell functions. *Immunol Rev*. 2013;256:160-176.

31. Bendris N, Lemmers B, Blanchard JM. Cell cycle, cytoskeleton dynamics and beyond: the many functions of cyclins and CDK inhibitors. *Cell Cycle*. 2015;14:1786-1798.

32. Badovinac VP, Haring JS, Harty JT. Initial T cell receptor transgenic cell precursor frequency dictates critical aspects of the CD8 (+) T cell response to infection. *Immunity*. 2007;26:827-841.

33. Kastenmüller W, Brandes M, Wang Z, Herz J, Egen JG, Germain RN. Peripheral prepositioning and local CXCL9 chemokine-mediated guidance orchestrate rapid memory CD8+ T cell responses in the lymph node. *Immunity*. 2013;38:502-513.

34. Darzynkiewicz Z, Staiano-Coico L, Melamed MR. Increased mitochondrial uptake of rhodamine 123 during lymphocyte stimulation. *Proc Natl Acad Sci U S A*. 1981;78:2383-2387.

35. Nusse M, Beisker W, Hoffmann C, Tarnok A. Flow cytometric analysis of G1- and G2/M-phase subpopulations in mammalian cell nuclei using side scatter and DNA content measurements. *Cytometry*. 1990;11:813-821.

36. Okhrimenko A, Grun JR, Westendorf K, et al. Human memory T cells from the bone marrow are resting and maintain long-lasting systemic memory. *Proc Natl Acad Sci U S A*. 2014;111:9229-9234.

37. Kamphorst AO, Pillai RN, Yang S, et al. Proliferation of PD-1+ CD8 T cells in peripheral blood after PD-1-targeted therapy in lung cancer patients. *Proc Natl Acad Sci U S A*. 2017;114:4993-4998.

38. Di Rosa F. Maintenance of memory T cells in the bone marrow: survival or homeostatic proliferation? *Nat Rev Immunol*. 2016;16:271.

39. Sercan Alp O, Radbruch A. The lifestyle of memory CD8(+) T cells. *Nat Rev Immunol*. 2016;16:271.

40. Villarroya-Beltri C, Gutiérrez-Vázquez C, Sánchez-Madrid F, Mittelbrunn M. Analysis of microRNA and protein transfer by exosomes during an immune synapse. *Methods Mol Biol*. 2013;1024:41-51.

41. Deng N, Weaver JM, Mosmann TR. Cytokine diversity in the Th1-dominated human anti-influenza response caused by variable cytokine expression by Th1 cells, and a minor population of uncommitted IL-2+IFNγ- Thpp cells. *PLoS ONE*. 2014;9:e95986.

SUPPORTING INFORMATION

Additional supporting information may be found online in the Supporting Information section at the end of the article.